



HAL
open science

Comparative analysis of ICA based Incoherent Target Decompositions for PolSAR data

Gabriel Vasile, Marco Congedo

► **To cite this version:**

Gabriel Vasile, Marco Congedo. Comparative analysis of ICA based Incoherent Target Decompositions for PolSAR data. IGARSS 2022 - IEEE International Geoscience and Remote Sensing Symposium, Jul 2022, Kuala Lumpur, Malaysia. 10.1109/IGARSS46834.2022.9883779 . hal-03727556

HAL Id: hal-03727556

<https://hal.science/hal-03727556v1>

Submitted on 19 Jul 2022

HAL is a multi-disciplinary open access archive for the deposit and dissemination of scientific research documents, whether they are published or not. The documents may come from teaching and research institutions in France or abroad, or from public or private research centers.

L'archive ouverte pluridisciplinaire **HAL**, est destinée au dépôt et à la diffusion de documents scientifiques de niveau recherche, publiés ou non, émanant des établissements d'enseignement et de recherche français ou étrangers, des laboratoires publics ou privés.

COMPARATIVE ANALYSIS OF ICA BASED INCOHERENT TARGET DECOMPOSITIONS FOR POLSAR DATA

*Gabriel Vasile**, *Marco Congedo**

* Grenoble-Image-sPeach-Signal-Automatics Lab, GIPSA-lab
Univ. Grenoble Alpes, CNRS / Grenoble INP, Grenoble, France
gabriel.vasile@grenoble-inp.fr, marco.congedo@grenoble-inp.fr

ABSTRACT

The Independent Component Analysis (ICA) has been recently introduced as a reliable alternative to identify canonical scattering mechanisms within PolSAR images. This paper addresses an overview of the most important aspects for applying such methods on real data. A new geometric classification algorithm is proposed by combining the polar decomposition and by adjusting the conventional k-means mean and distance with their counterpart on the Riemannian manifold. This algorithm is tested using P-band airborne PolSAR data acquired for the ESA campaign TropiSAR campaign.

Index Terms— Incoherent Target Decomposition, ICA, PolSAR, data analysis

1. INTRODUCTION

Polarimetric Synthetic Aperture Radar (SAR) images can be used for several applications, for example for land cover classification. With current SAR sensors being able to emit or receive two orthogonal polarizations, the polarimetric target decompositions are PolSAR image interpretation techniques relying on the study of the interaction between the targeted area and the transmitted waveform. In this context, the Incoherent Target Decomposition (ICTD) theory assumes that the scattering process is a combination of coherent speckle and random vector scattering effects [1, 2]. Polarimetric target decomposition is a PolSAR image interpretation technique that relies on the analysis of the interaction between the illuminated area and the transmitted waveform, considering each polarimetric state of the latter. More specifically, it enables the description of an image cell as a sum of canonical scattering mechanisms (also called as target vectors) making it more intuitive to understand the behavior of the clutter and therefore to analyze it [1].

In the remaining parts of this paper, Section 2 is dedicated to a short review of the ICA-ICTD framework and to the introduction of a new classification algorithm, while Section 3

presents results obtained using real PolSAR data. Lastly, Section 4 provides some directions for further investigation.

2. INCOHERENT TARGET DECOMPOSITION TECHNIQUES FOR POLSAR DATA

ICTD algorithms can be split in two stages: the decomposition of an image pixel into basic target vectors and the correct retrieval of quantitative information from them (parametrization). In this paper, we propose a comparative analysis of three ICTD techniques: Cloude and Pottier's H/α , Touzi's TSVM and ICA based ICTD.

The combined use of the Eigenvector approach with Cloude and Pottier's parametrisation gave rise to one of the most employed and most traditional classification schemes in PolSAR data analysis, the H/α feature space [3]. The entropy, H , measures the degree of randomness of the scattering phenomenon, given as a function of the eigenvalues of the coherence matrix. Each eigenvector correspond to a scattering mechanism within the image cell and therefore each one will provide a different α angle. The authors in [3] state that the best estimate of such parameter to represent the image cell is an weighted average based on the eigenvalues of the coherence matrix.

The parameters H and α are plotted in a plane, originating the so called H/α feature space. Upon the introduction of the aforementioned method, Cloude and Pottier suggested the partitioning of the plane in 9 regions, based on the polarimetric behavior of known type of natural phenomena. Therefore, once the H and the average α parameters are extracted from the target polarimetric signature, it is straightforward to classify it as one of the corresponding type of scattering mechanisms. Many works are based on such method, from geophysical parameters inversion algorithms (in varied regions from the globe) to detection and classification algorithms. Having a remarkable correspondence to ground truth, the usage of this unsupervised technique has had very few improvements since its conception. It has been shown in [4] that the Independent Component Analysis (ICA) provides additional information: unconstrained by the orthogonality condi-

Thanks to the French Aerospace Lab for providing the PolSAR data.

tion between the estimated scattering mechanisms that compose the PolSAR clutter under analysis, ICA is not subject to the unfeasible region in the H/α plane, increasing the range of possible natural phenomena depicted in this feature space.

In [5], a novel strategy to polarimetric ICTD was introduced by selecting the Independent Component Analysis (ICA) to identify the canonical scattering mechanisms within an image cell. The proposed ICA was able to retrieve non-orthogonal scatterer types [6, 4]. This ICA-ICTD decomposition can be applied either locally (inside a sliding neighborhood) or globally (using a redefined classification map).

In the local approach, by applying the MMSE filter [7] on each of the ICA derived rotation invariant scattering vectors, we have shown in [8] that spatial resolution can be better preserved with respect to the conventional PolSAR boxcar speckle filter.

The ICA based ICTD decomposition is based on the estimation of the mixing matrix \mathbf{A} (Eq. 1). There are several criteria for determining the elements of \mathbf{A} in order to ensure the mutual independence of the sources in \mathbf{s} . The common factor for all the applied methods is the assumption that at most one of the sources is Gaussian.

$$\mathbf{k}^c(i, j) = \begin{bmatrix} A_{11}^c & A_{12}^c & A_{13}^c \\ A_{21}^c & A_{22}^c & A_{23}^c \\ A_{31}^c & A_{32}^c & A_{33}^c \end{bmatrix} \cdot \begin{bmatrix} s_1^c(i, j) \\ s_2^c(i, j) \\ s_3^c(i, j) \end{bmatrix} = \mathbf{A}^c \mathbf{s}^c(i, j) \quad (1)$$

The selected Complex Fast-ICA algorithm is based on a *bottom-up* approach: emphasizing the non-gaussianity of the sources by maximizing an arbitrary nonlinear contrast function (Eq. 2) whose extrema coincides with the independent component.

$$J_G(\mathbf{w}) = \mathbf{E}\{G(|\mathbf{w}^H \mathbf{x}|^2)\} \quad (2)$$

The performances of the algorithm depend strongly on the choice of the nonlinear function $G(y)$, which is supposed to be suited to the particular application. Therefore, here we have used the kurtosis criterion in deriving independent target vectors:

$$G_1(y) = \frac{1}{2}y^2. \quad (3)$$

In this case, the contrast functions becomes essentially a measure of the fourth statistical moment of the source. As its value in case of the Gaussian variable equals zero, by maximizing the kurtosis of each of the sources, we ensure their independence.

The result of the incoherent target decomposition is the set of target vectors representing elementary scatterers and a set of scalars, providing their proportion in the total scattering. In our case, the target vectors of the independent scatterers are the columns of the estimated mixing matrix $\mathbf{A} = \mathbf{W}^H$. The contribution to the total backscattering (m) is computed as a square root of the maximal eigenvalue of the derived Graves matrix.

Being based on Kennaugh-Huynen condiagonalization projected onto the Pauli basis, the TSVM [9] allows parametrization of the target vector in terms of rotation angle (ψ), maximum amplitude (m), target helicity (τ_m), symmetric scattering type magnitude (α_s) and symmetric scattering type phase (Φ_{α_s}), among which the last four are roll-invariant:

$$\mathbf{k} = m|\mathbf{k}|_m e^{j\Phi_s} \begin{bmatrix} 1 & 0 & 0 \\ 0 & \cos 2\psi & -\sin 2\psi \\ 0 & \sin 2\psi & \cos 2\psi \end{bmatrix} \begin{bmatrix} \cos \alpha_s \cos 2\tau_m \\ \sin \alpha_s e^{j\Phi_{\alpha_s}} \\ -j \cos \alpha_s \sin 2\tau_m \end{bmatrix}. \quad (4)$$

Using these parameters, it is eventually possible to represent the obtained independent target vectors on either symmetric or non-symmetric target Poincaré sphere. In the ICA case, they do not necessarily form an orthogonal basis.

2.1. Global approach: classification on the Riemannian manifold using the polar decomposition

In the global approach, one may think to classify directly the mixing matrices derived by the Fast-ICA, however there is not a well established metric for the general linear group. Instead we propose here to consider the polar decomposition of the original 2×2 scattering matrices, following [10].

The right polar decomposition of scatter matrix \mathbf{S} is given by:

$$\mathbf{S} = \mathbf{U}\mathbf{P}, \quad (5)$$

where \mathbf{U} is a unitary matrix and $\mathbf{S} = \sqrt{\mathbf{S}^H \mathbf{S}}$ is a Hermitian matrix. The unitary factor is unique if \mathbf{S} is non-singular, which is the practical case of PolSAR data due to the presence of speckle and thermal noise in the scattering matrices.

Further on, we concentrate on the Hermitian factor \mathbf{P} and we discard the unitary factor from Eq. 5. Therefore, each pixel of the PolSAR image yields a Hermitian matrix \mathbf{P}_i lying on the Riemannian manifold of positive matrices [11].

Exploiting this geometry, we first replace the complex multilooking by computing the Riemannian barycenter within a local neighborhood of the current pixel in order to remove the speckle. Second, we cluster the pixels using, for example, a modified k-means algorithm, where the mean and distance are replaced by their counterpart on the Riemannian manifold of positive definite matrices.

Specifically, in this manifold we adopt the widely used affine-invariant metric for two tangent vectors \mathbf{V} and \mathbf{W} , defined by

$$\langle \mathbf{V}, \mathbf{W} \rangle_P = \text{Tr}(\mathbf{P}^{-1} \mathbf{V} \mathbf{P}^{-1} \mathbf{W}). \quad (6)$$

It follows the distance between two points on the manifold (positive definite matrices), given by

$$d^2(\mathbf{X}, \mathbf{Y}) = \|\log(\mathbf{X}^{-1/2} \mathbf{Y} \mathbf{X}^{1/2})\|_F^2, \quad (7)$$

and the barycenter (geometric mean) of a set of points, which is the unique solution of

$$B = \underset{i}{\text{argmin}} \sum d^2(\mathbf{X}_i, \mathbf{G}). \quad (8)$$

3. POLSAR EXPERIMENTAL RESULTS

The PolSAR dataset was acquired by the French Aerospace Lab (ONERA), in 2009, over the French Guiana, in the frame of the ESA campaign TropiSAR. With local processing, Fig. 2-(a),(b),(c),(d) shows the Touzi's roll invariant TSVM parameters computed by ICA MMSE speckle filtering, as compared to the ones obtained by applying the boxcar filter and PCA from Fig. 1-(a),(b),(c),(d).

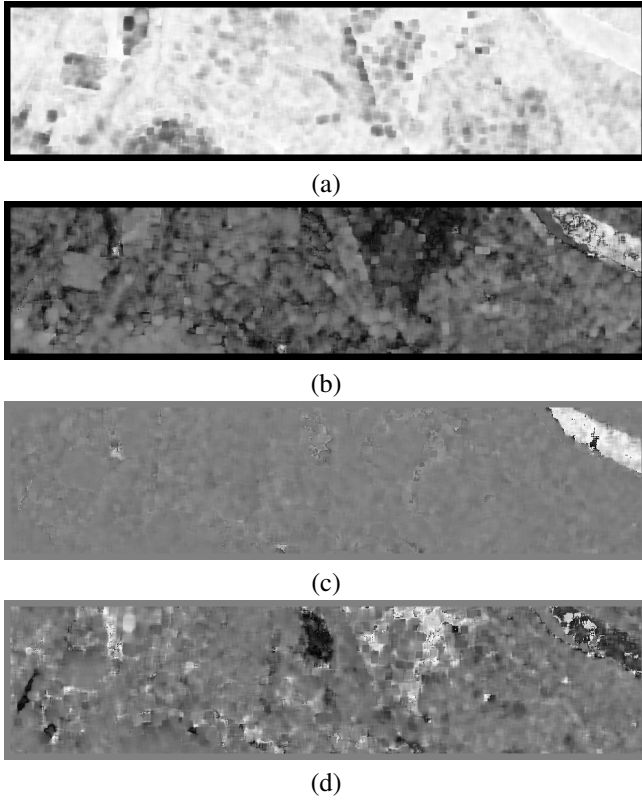


Fig. 1. Paracou P-band airborne dataset, TSVM parameters after PCA boxcar speckle filtering: (a) entropy, (b) symmetric scattering type magnitude, (c) helicity and (d) symmetric scattering type phase.

As an example, we propose to analyse the results by representing the derived TSVM parameters of symmetric targets on the Poincaré sphere (helicity equal 0). It can be observed in Fig. 3-(a),(b) that the second and the third most dominant mechanism (represented in blue and green, respectively) occupy different position onto the sphere, thus meaning that the non-orthogonality of ICA will produce different mechanisms, indeed.

Regarding the global approach, we propose in Fig. 4 a comparison between complex multilooking and Riemannian barycenter as an estimate of the local 2×2 Hermitian factor of scattering matrix. The size of the local neighborhood is 7×7 . One can observe in Fig. 4-(b) that derived result is more robust to the inherent speckle noise.

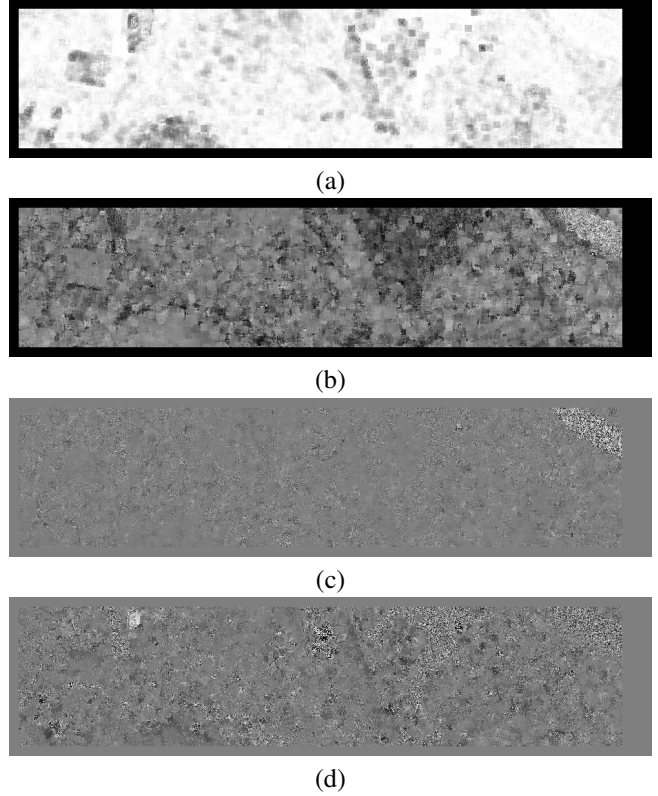


Fig. 2. Paracou P-band airborne dataset, TSVM parameters after ICA MMSE speckle filtering: (a) entropy, (b) symmetric scattering type magnitude, (c) helicity and (d) symmetric scattering type phase.

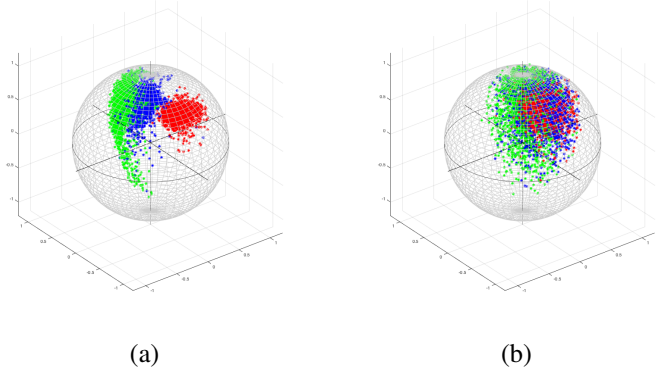


Fig. 3. Paracou P-band airborne dataset, Poincaré sphere representation of symmetric targets: (a) PCA with boxcar, (b) MMSE with ICA.

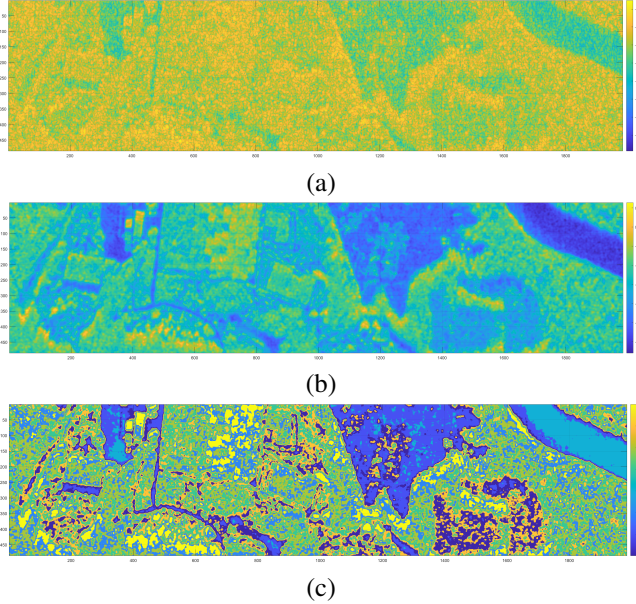


Fig. 4. Paracou P-band airborne dataset, 7×7 local neighborhood: (a) first element of the scattering matrix $|S_{1,1}|^2$ (in dB) obtained by complex multilooking, (b) first element of the Hermitian factor $|P_{1,1}|^2$ (in dB) derived as the local barycenter and (c) Riemannian k-means classification map.

Finally, we illustrate in Fig. 4-(c) the classification map, in slant range, obtained using the proposed modified k-means classifier with random initialization and $N = 8$ classes. This can be re-sampled in ground range as proposed in [12].

4. CONCLUSION

This paper presented an overview of the most important aspects for applying ICA based incoherent target decompositions on real PolSAR data. Based on the coupling between the polar decomposition and the Riemannian k-means clustering, we have proposed a new classification algorithm for the global analysis of such data. Results have been illustrated using P band airborne PolSAR data over forested areas.

Further developments will be addressed to take into account also the left polar decomposition and to combine it in the final classification result.

5. REFERENCES

- [1] S. R. Cloude and E. Pottier, “A review of target decomposition theorems in radar polarimetry,” *IEEE Transactions on Geoscience and Remote Sensing*, vol. 32, no. 6, pp. 498–518, 1996.
- [2] R. Touzi, “Speckle effect on polarimetric target scattering decomposition of SAR imagery,” *Canadian Journal of Remote Sensing*, vol. 33, no. 1, pp. 60–68, 2007.
- [3] S. R. Cloude and E. Pottier, “An entropy based classification scheme for land applications of polarimetric SAR,” *IEEE Transactions on Geoscience and Remote Sensing*, vol. 35, no. 1, pp. 68–78, 1997.
- [4] L. Pralon, G. Vasile, M. Dalla-Mura, and J. Chanussot, “Evaluation of the new information in the H/α feature space provided by ICA in PolSAR data analysis,” *IEEE Transactions on Geoscience and Remote Sensing*, vol. 55, no. 12, pp. 6893–6909, 2017.
- [5] N. Besic, G. Vasile, J. Chanussot, and S. Stankovic, “Polarimetric incoherent target decomposition by means of independent component analysis,” *IEEE Transactions on Geoscience and Remote Sensing*, vol. 53, no. 3, pp. 1236–1247, 2015.
- [6] L. Pralon, G. Vasile, M. Dalla-Mura, J. Chanussot, and N. Besic, “Evaluation of ICA-based ICTD for PolSAR data analysis using a sliding window approach: convergence rate, gaussian sources, and spatial correlation,” *IEEE Transactions on Geoscience and Remote Sensing*, vol. 54, no. 7, pp. 4262–4271, 2016.
- [7] J. S. Lee, T. L. Ainsworth, Y. Wang, and K. S. Chen, “Polarimetric SAR speckle filtering and the extended sigma filter,” *IEEE Transactions on Geoscience and Remote Sensing*, vol. 53, no. 3, pp. 1150–1160, 2015.
- [8] G. Vasile, “Independent component analysis based incoherent target decompositions for polarimetric SAR data - practical aspects,” in *Proceedings of IEEE International Geoscience and Remote Sensing Symposium, Valencia, Spain*, 2018, pp. 5859–5862.
- [9] R. Touzi, “Target scattering decomposition in terms of roll-invariant target parameters,” *IEEE Transactions on Geoscience and Remote Sensing*, vol. 45, no. 1, pp. 73–84, 2007.
- [10] J.C. Souyris and C. Tisson, “Polarimetric analysis of bistatic SAR images from polar decomposition: A quaternion approach,” *IEEE Transactions on Geoscience and Remote Sensing*, vol. 45, no. 9, pp. 2701–2714, 2017.
- [11] R. Bhatia and J. Holbrook, “Riemannian geometry and matrix geometric means,” *Linear Algebra and its applications*, vol. 413, no. 2, pp. 594–618, 2005.
- [12] A. Julea, G. Vasile, I. Petillot, E. Trouve, M. Gay, J.M. Nicolas, and P. Bolon, “Simulation of SAR images and radar coding of georeferenced information for temperate glacier monitoring,” in *Proceedings of the International Conference on Optimization of Electrical and Electronic Equipment, Brasov, Romania*, 2006, vol. 4, pp. 175–180.